Colloid Polym Sci (2006) 284: 497–505
DOI 10.1007/s00396-005-1410-6

ORIGINAL CONTRIBUTION

Hossein Tavana
Dietmar Appelhans
Rong-Chuan Zhuang
Stefan Zschoche
Karina Grundke
Michael L. Hair
A. Wilhelm Neumann

Determination of accurate surface tensions of maleimide copolymers containing fluorinated side chain from contact angle measurements

Received: 22 July 2005
Accepted: 18 October 2005
Published online: 29 November 2005

H. Tavana · M. L. Hair ·
A. W. Neumann (✉)
Department of Mechanical
and Industrial Engineering,
University of Toronto,
5 King's College Road,
Toronto, Ontario, M5S 3G8, Canada
e-mail: neumann@mie.utoronto.ca
Tel.: +1-416-9781270
Fax: +1-416-9787753

D. Appelhans · R.-C. Zhuang ·
S. Zschoche · K. Grundke
Leibniz Institute for Polymer Research,
Hohe Strasse 6,
01069 Dresden, Germany

Abstract Surface energetics of two fluorinated maleimide copolymers containing fluorinated side chain, i.e., poly(ethene-*alt*-*N*-(4-(perfluoroheptylcarbonyl)aminobutyl)maleimide) (ETMF) and poly(octadecene-*alt*-*N*-(4-(perfluoroheptylcarbonyl)aminobutyl)maleimide) (ODMF), are studied by contact angle measurements with 10 liquids consisting of fairly bulky molecules. Because of the inertness of octamethylcyclotetrasiloxane (OMCTS) and decamethylcyclopentasiloxane (DMCPS) molecules, their contact angles are used to determine the surface tension of the two polymers. It is found that other liquids show specific interactions with the ETMF films, and their contact angles deviate from a smooth curve that represents the surface tension of ETMF, i.e., 11.00 mJ/m^2. On ODMF surfaces, only OMCTS and DMCPS yield useful contact angles. Other liquids either dissolve the polymer film or show a slip-stick pattern. This finding is discussed in terms of interactions between segments of the polymer chains and the test liquids. OMCTS and DMCPS are suggested as the appropriate probe liquids, meeting specific criteria necessary for the determination of accurate surface tension of fluoropolymers.

Keywords Contact angles · Solid surface tensions · Maleimide copolymers · Specific interactions · Structure–property relationship

Introduction

Surface properties of polymers including surface tensions are extremely important because of the numerous applications they find in a wide variety of biological and industrial problems, where wetting of a solid surface by a liquid is of interest. Orthopedic technology, lubrication, paint, coating, and paper industries are a few examples. Because surface energies involving a solid phase cannot be measured directly, contact angle measurements are widely used as an indirect approach for this purpose. Determination of solid surface tensions from contact angles relies on Young's equation [1] that states the mechanical equilibrium of a liquid drop under the action of the three interfacial tensions, i.e., liquid–vapor (γ_{lv}), solid–vapor (γ_{sv}), and solid–liquid (γ_{sl}):

$$\gamma_{lv}\cos\theta = \gamma_{sv} - \gamma_{sl}, \tag{1}$$

where θ, i.e., Young's contact angle, and γ_{lv} are measurable quantities. The need for an additional relation to estimate solid surface tensions has motivated many studies [2–8]. From contact angle measurements with a large number of liquids on one and the same polymeric solid surface, it was shown that $\gamma_{lv}\cos\theta$ changes smoothly with γ_{lv}. Parallel

curves are obtained by replacing the solid, each curve representing the surface tension of the polymer film in question. This implies that:

$$\gamma_{lv}\cos\theta = f(\gamma_{lv}, \gamma_{sv}). \quad (2)$$

Combining this relation with the Young equation yields:

$$\gamma_{sl} = F(\gamma_{lv}, \gamma_{sv}). \quad (3)$$

Based on this relation, an "equation of state for the interfacial tensions" was developed:

$$\gamma_{sl} = \gamma_{lv} + \gamma_{sv} - 2\sqrt{\gamma_{lv}\gamma_{sv}}\,e^{-\beta(\gamma_{lv}-\gamma_{sv})^2}, \quad (4)$$

where β is an empirical constant with an average value of 0.000125 $(mJ/m^2)^{-2}$ [9]. If Eqs. 1 and 4 are combined, an explicit relation between contact angle and the solid surface tension, γ_{sv}, is obtained:

$$Cos\theta = -1 + 2\sqrt{\frac{\gamma_{sv}}{\gamma_{lv}}}\,e^{-\beta(\gamma_{lv}-\gamma_{sv})^2}. \quad (5)$$

With the values of θ and γ_{lv} known from experiments, β and γ_{sv} can be obtained using a multivariable optimization technique [9].

Examining many solid–liquid systems showed that contact angles usually do not fall perfectly on the smooth curves of $\gamma_{lv}\cos\theta$ vs γ_{lv} but scatter around the curves (see Figs. 13 and 14 in [10]). Although the typical scatter is ~1–2°, some systems do show even larger deviations from smooth curves. The existence of deviations introduces an element of uncertainty in the determination of accurate surface tension of solids. As an example, a deviation of ~5° in the contact angles results in an error of ~2 mJ/m^2 in the calculated value for the solid surface tension. Therefore, it was crucial to find out the underlying causes. This problem was addressed in earlier studies, and the highlights are presented below.

It was shown that the contact angle deviations are not an artifact of experimental procedures and must have physical causes. This was achieved by (a) accurate reproducibility of contact angles of a series of *n*-alkanes on Teflon AF 1600 films [11] and (b) a systematic study of the contact angles on polymeric films of different thickness prepared by spin-coating and dip-coating techniques [12].

Contact angles of 10 liquids consisting of nearly spherical, rigid, and nonflexible molecules (mean molecular diameter ~0.61–0.9 nm) on Teflon AF 1600 surfaces fall on a smooth curve corresponding to γ_{sv}=13.61±0.07 mJ/m^2 and β=0.000116 $(mJ/m^2)^{-2}$ (circles in Fig. 1) [13]. The value of β is in a good agreement with the value obtained before [9]. Considering that the average contact angle deviation for these liquids is very small (±0.24°), it was suggested that these liquids do not undergo specific interactions, e.g., liquid penetration or reorientation of liquid molecules or polymer chains, upon contact with Teflon films. Thus, the value of γ_{sv}=13.61 mJ/m^2 was considered as the surface tension of Teflon AF 1600 surfaces [13]. These liquids were labeled "liquids with bulky molecules" because of their molecular size and shape. On the other hand, contact angles of six other liquids with fairly bulky molecules but containing exposable electronegative moieties of oxygen and nitrogen fall ~3° below this curve (triangles in Fig. 1). These results were interpreted in terms of a nonuniform charge distribution over liquid molecules as well as in the polymer chains, resulting in a reorientation of liquid molecules close to the solid surface and changing the solid–liquid interfacial tension from the ideal situation.

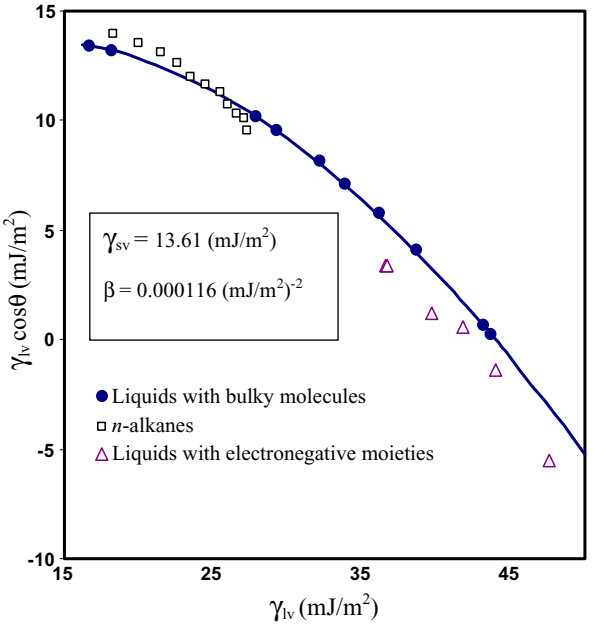

Fig. 1 $\gamma_{lv}\cos\theta$ vs γ_{lv} for three groups of liquids on Teflon AF 1600 films. While liquids with bulky molecules fall on the γ_{sv}=13.61 mJ/m^2 curve, contact angles of *n*-alkanes and liquids containing electronegative moieties show deviations from that curve

Moreover, contact angles of a series of *n*-alkanes, i.e., *n*-hexane to *n*-hexadecane, on Teflon AF 1600 surfaces deviate from the γ_{sv}=13.61 mJ/m^2 curve in a complicated fashion [11] (rectangles in Fig. 1). The contact angles of the liquids with short chains fall above the curve, where *n*-hexane yields the largest deviation with −3.52°. Then the deviations decrease so that the contact angles of *n*-decane, *n*-undecane, and *n*-dodecane fall very close to that curve. Moving to the *n*-alkanes with longer chains, the deviations change sign and increase again to +2.07° for *n*-hexadecane. It was suggested that adsorption of vapor of short-chain *n*-alkanes onto the polymer film before the drop starts advancing and a substrate-induced parallel alignment of molecules of long-chain *n*-alkanes near the solid surface are the most likely explanations for the corresponding contact angle deviations. Parallel reorientation of *n*-alkanes

molecules close to solid surfaces has been reported in the literature [14–18]. A combination of these two effects caused the contact angles of the three liquids in the middle of the series to fall very close to the curve.

To find out whether contact angle measurements on other fluoropolymer films would yield similar results, poly (2,2,3,3,4,4,4-heptafluorobutyl methacrylate) (EGC-1700) was selected for a second series of experiments [19]. This polymer is different somewhat from Teflon AF 1600 in terms of chemical composition and chain structure, allowing the study of the influence of such parameters on the contact angles. It was shown that the γ_{sv} values obtained from contact angles of liquids with bulky molecules were not consistent and varied from 13.82 mJ/m^2 calculated for octamethylcyclotetrasiloxane (OMCTS) to 16.10 mJ/m^2 for 1-bromonaphthalene. To elucidate the mechanisms that cause such variations in γ_{sv} and therefore to determine the surface tension of this polymer, three issues were considered: molecular structure of the test liquids and the polymer, receding contact angle patterns, and contact angle hysteresis of the liquids. X-ray Photoelectron Spectroscopy (XPS) analysis of EGC-1700 films showed that in addition to the fluorine-containing moieties, polymer groups with a moderate polarity might also be exposed to the surface film upon contact with a liquid. Moreover, molecular modeling shows that except for OMCTS and decamethylcyclopentasiloxane (DMCPS), the liquids are not completely inert either because they contain double bonds or exposable electronegative substituents. Therefore, upon contact between a noninert liquid and the polymer film, the polymer chains are reoriented such that some groups less hydrophobic than CF_2 and CF_3 are also exposed towards the liquid phase. Consequently, the solid–liquid interfacial tension at the three-phase line region is not determined solely by fluorine-containing moieties. Therefore, the contact angles of these liquids do not yield the accurate surface tension of EGC-1700. The fact that only OMCTS and DMCPS yielded time-independent receding angles and also small contact angle hysteresis confirmed that the interactions between their molecules and the polymer chains are nonspecific, i.e., no significant change in the arrangement of polymer chains or liquid molecules upon contact. Therefore, the surface tension of EGC-1700 was determined from their contact angles. The average is γ_{sv}=13.84 mJ/m^2.

Contact angles of *n*-alkanes were also studied on EGC-1700 films, and a pattern similar to that shown in Fig. 1 (*n*-alkanes/Teflon AF 1600 systems) was obtained. However, the extent of deviations in the contact angles is different, i.e., −1.07° for *n*-hexane and +2.56° for *n*-hexadecane.

A series of criteria necessary for the test liquids to determine solid surface tensions accurately was concluded from contact angle results: The liquids should be completely inert (without unsaturated or electronegative moieties), with extremely low vapor pressure, with bulky and nonflexible molecules, and without propensity for electronegative moieties in the polymer surface. OMCTS and DMCPS were suggested as the only two liquids that meet all these conditions. To investigate the above findings further and to establish whether the proposition of using liquids with bulky siloxane rings such as OMCTS and DMCPS for the determination of surface tension of fluoropolymers is valid, contact angle measurements were performed with a group of liquids consisting of bulky molecules on two maleimide copolymers containing fluorinated side groups that possess chemical composition and molecular structure different from Teflon AF 1600 and EGC-1700 (see below). It is noted that some contact angle measurements with *n*-alkanes on these two fluoropolymers show slip-stick patterns, requiring very different considerations. These results will therefore be presented elsewhere (Tavana et al., unpublished data).

Materials and methods

Solid surfaces

Silicon wafers ⟨100⟩ (Silicon Sense, Naschua, N.H.; thickness 525±50 μm) were selected as the substrate because of their smoothness and rigidity. The coating materials poly (ethene - *alt* - *N* - (4 - (perfluoroheptylcarbonyl)aminobutyl) maleimide) (ETMF) and poly(octadecene - *alt* - *N* - (4 - (perfluoroheptylcarbonyl) aminobutyl) maleimide) (ODMF) were provided by the Leibniz Institute for Polymer Research (IPF), Dresden, Germany. The repeat unit of the two polymers is illustrated in Fig. 2. Both polymers possess a *N*-(4-(perfluoroheptylcarbonyl)aminobutyl) side chain. In addition, ODMF contains a second side chain, i.e., *n*-hexadecyl. XPS analysis showed a preferred alignment of the fluorinated side groups on the upper layer of ETMF and ODMF films. Details about the XPS analysis, synthesis, bulk, and surface properties of these copolymers can be found in [20].

Solutions of ODMF and ETMF (2 wt%) were prepared in tetrahydrofuran (99.9+% pure) and 1,1,1,3,3,3,-hexafluoro-2-propanol (99.8% pure), respectively. The surfaces were prepared by a dip-coating technique [13]. To remove the solvent from the coating films and to improve adhesion of the polymers to the substrates, the surfaces were annealed in an oven for 24 h. The annealing temperatures for ODMF and ETMF polymer films were 85 and 120°C, respectively, i.e., about 20°C above their glass transition temperature. This technique usually yields high-quality films with a thickness of several hundred nanometers. Atomic force microscopy (AFM) analysis showed that RMS mean roughness for the dip-coated ODMF and ETMF films are ~1.3 and ~0.4 nm, respectively.

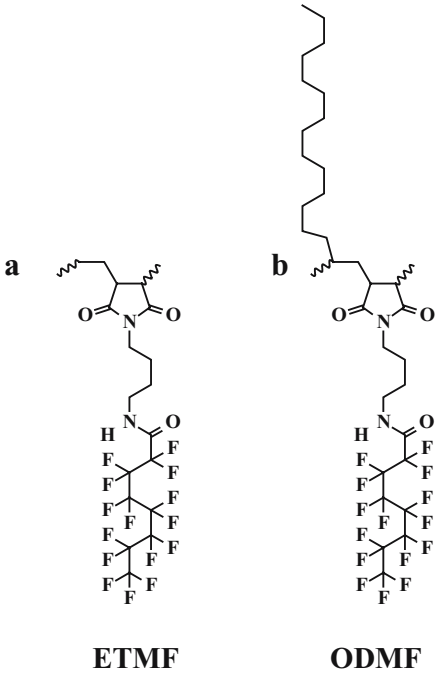

Fig. 2 Repeat unit of the two copolymers. **a** Poly(ethene-*alt*-*N*-(4-(perfluoroheptylcarbonyl)aminobutyl)maleimide) (ETMF). **b** Poly(octadecene-*alt*-*N*-(4-(perfluoroheptylcarbonyl)aminobutyl)maleimide) (ODMF)

Test liquids

The following liquids with bulky molecules were selected for the contact angle study: OMCTS, DMCPS, *p*-xylene, *o*-xylene, *cis*-decalin, tetralin, diethyl phthalate, methyl salicylate, lepidine (4-methylquinoline), and 1-bromonaphthalene. All the liquids were purchased from Sigma-Aldrich Co. (Oakville, Ontario, Canada) at the highest purity available.

Methods and procedures: axisymmetric drop shape analysis-profile

In principle, the shape of a drop is determined by the balance between gravity and interfacial tension and is defined by the Laplace equation of capillarity. Assuming the experimental drop profile to be axisymmetric and Laplacian, axisymmetric drop shape analysis-profile (ADSA-P) finds the theoretical drop profile that best matches the drop profile extracted from the image of a real drop. From the best match, contact angles, volume and surface area of the drop, the three-phase contact radius, and the liquid–vapor interfacial tension are determined. Details can be found elsewhere [21].

The contact angles reported in this paper were determined by sessile drop experiments. An initial drop was deposited on the solid surface from above. Then, a motorized syringe was operated to pump the liquid steadily into the drop so that low-rate advancing contact angles were obtained. The images of the drop were recorded during the experiment and analyzed by ADSA-P afterwards. More details can be found in [13].

Results and discussion

Contact angle measurements were performed with the liquids listed above on ETMF and ODMF films. To ensure the reproducibility of the contact angles, measurements were repeated at least five times for each liquid, each on a freshly prepared solid surface. As an example, contact angles of DMCPS on ETMF films obtained from five different experiments are given in Table 1. The 95% confidence limits for the contact angles are also included. Since contact angles were constant during each run, they were averaged to yield a mean value for the experiment. Thus, the contact angle of DMCPS on ETMF surfaces is 58.16±0.09°. The γ_{sv} values obtained from each contact angle are also given in Table 1.

Surface tension of ETMF films from contact angle measurements

Table 2 presents the surface tension of the test liquids and their contact angles on ETMF surfaces. The values of solid surface tension calculated from each pair of γ_{lv} and θ_a are also given. As seen, the γ_{sv} values vary from 10.88 mJ/m^2 calculated for OMCTS to 12.94 mJ/m^2 for methyl salicylate. The fact that similar results had been obtained for EGC-1700 surfaces [19] suggests that the mechanism responsible for variations in the γ_{sv} values may be similar. Thus, a similar strategy is employed to investigate the surface tension of ETMF films, i.e., considering molecular structure of the liquids and the polymer surface, receding contact angle patterns, and the contact angle hysteresis of the test liquids.

OMCTS and DMCPS are inert in the sense explained previously [13, 19], but the other test liquids are not

Table 1 Advancing contact angles of DMCPS on ETMF surfaces and the corresponding solid surface tension values

Run number	Advancing contact angle, θ_a (°)	γ_{sv} (mJ/m^2)
1	58.24±0.03	11.09
2	58.07±0.04	11.13
3	58.21±0.07	11.10
4	58.18±0.03	11.11
5	58.11±0.05	11.12
Mean	58.16±0.09	11.11±0.02

ETMF poly(ethene-*alt*-*N*-(4-(perfluoroheptylcarbonyl)aminobutyl) maleimide)

Table 2 Advancing contact angles of liquids with bulky molecules on ETMF films. The calculated values for solid surface tension from each pair of γ_{lv} and θ_a are also given

Liquid	γ_{lv} (mJ/m^2)	θ_a (°)	γ_{sv} (mJ/m^2)
OMCTS	18.20	57.70±0.08	10.88
DMCPS	18.77	58.16±0.09	11.11
p-Xylene	27.90	75.60±0.23	11.62
o-Xylene	29.30	77.50±0.17	11.71
cis-Decalin	32.16	80.87±0.29	11.95
Tetralin	36.15	84.67±0.12	12.42
Diethyl phthalate	36.67	86.40±0.18	12.05
Methyl salicylate	38.71	86.38±0.11	12.94
Lepidine	43.20	91.36±0.22	12.91
1-Bromonaphthalene	43.70	92.05±0.17	12.87

OMCTS octamethylcyclotetrasiloxane, *DMCPS* decamethylcyclopentasiloxane

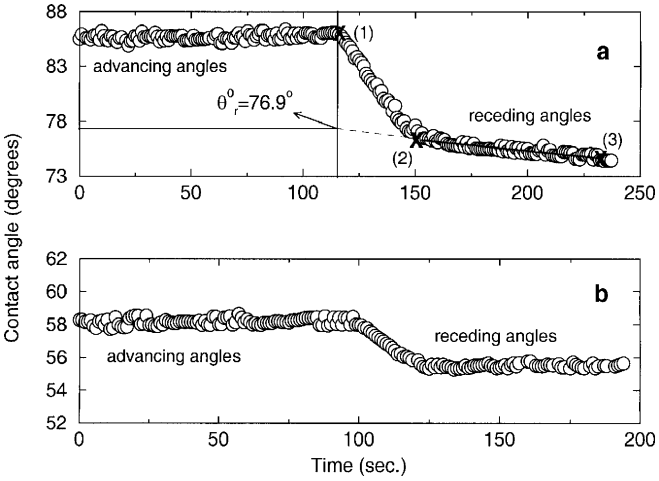

Fig. 3 Contact angles of methyl salicylate (**a**) and DMCPS (**b**) on ETMF films. The receding angles of DMCPS are constant, while methyl salicylate shows time-dependent receding angles

completely inert due to the presence of unsaturated bonds or exposable electronegative moieties that bring about an uneven charge distribution. Therefore, it is plausible that due to mobility of the long side chains of ETMF, groups other than CF_2 and CF_3—such as the aliphatic hydrocarbon segment (butyl) or possibly the amide group of the side chain—can be exposed towards the liquid phase upon advancing of the drop front of a noninert liquid. The contribution of these moieties at the three-phase line region causes the γ_{sl} and consequently θ_a, to be less than their corresponding "ideal" values [11]. In the "ideal" situation, only fluorine-containing moieties would be exposed to the surface film including the three-phase line region. Change in arrangement of the chains of polymer surfaces upon contact with a liquid is well established [22–28]. This is facilitated by a decrease in the solid–liquid interfacial tension. On the other hand, inertness of OMCTS and DMCPS suggests that the solid–liquid molecular interactions must be nonspecific, i.e., no significant change in the orientation of liquid molecules or organization of the side chains at the top layer of the polymer film. It should be noted that a major rearrangement in the chains of ETMF is less likely to occur. This will be explained below.

Receding contact angle patterns and contact angle hysteresis of the liquids support this proposition. Except for OMCTS and DMCPS, the receding angles of all the other liquids on ETMF films depend on the contact time between solid and liquid. This is shown in Fig. 3 for methyl salicylate (a) and DMCPS (b). The explanation for the time dependence of receding angles is complicated. Penetration of liquid molecules into the polymer matrix, retention of liquid molecules on the surface, and change in the alignment of the side chain segments might all play equally important roles, which cannot be distinguished easily. This will be discussed in detail below. For these liquids, the contact angle hysteresis was obtained as follows.

Lam et al. [29] studied the contact angles of a series of *n*-alkanes and *n*-alcohols on the fluoropolymer FC-732 surfaces. The receding angles for all solid–liquid systems were dependent on the contact time between solid and liquid. It was suggested that the polymer film might be modified through sorption-type processes (see [30] for more information about liquid sorption by a polymer film). To determine the receding angles that could be ideally obtained on a FC-732 film in the absence of sorption, the receding angles were extrapolated back to the point where the motor had been reversed [point (1) in Fig. 3a], i.e., to the beginning of decrease in the drop volume. Fig. 3a shows an example of this strategy for methyl salicylate. Contact angle hysteresis was then calculated as the difference between advancing and the extrapolated receding angles. Table 3 presents the results for the extrapolated receding angles (θ_r^o) and contact angle hysteresis (θ_{hyst}^0). A close scrutiny of the results in this table elucidates that the contact angle hysteresis (θ_{hyst}^0) for the liquids containing

Table 3 Extrapolated receding contact angles and contact angle hysteresis (degrees) for liquids with bulky molecules on ETMF surfaces

Liquid	θ_r^o (°)	$\theta_{hyst.}^o$ (°)
p-Xylene	71.5	4.1
o-Xylene	74.0	3.5
cis-Decalin	77.2	3.7
Tetralin	80.0	4.7
Diethyl phthalate	76.4	10.0
Methyl salicylate	76.8	9.4
Lepidine	81.9	9.5
1-Bromo-naphthalene	83.0	9.1

electronegative moieties (the last four in Table 3) is about twice as large as for those with molecules that contain double bonds (the first four in Table 3). This may raise the question of comparing the slopes of the regression lines for the receding angles of these liquids [e.g., from points (2) to (3) in Fig. 3a for methyl salicylate] because it determines the extrapolated receding angles. This will be discussed in more detail below.

On the other hand, since OMCTS and DMCPS show constant receding angles, the hysteresis in their contact angle was simply obtained as the difference between advancing and receding angles, and the results are given in Table 4. The fact that OMCTS and DMCPS yield constant receding angles and also a very small contact angle hysteresis indicates no significant ordering or rearrangement in the polymer or liquid molecules occur.

The above investigation of the molecular composition and configuration for the test liquids and the polymer surface, receding contact angle patterns and contact angle hysteresis, suggests that the correct surface tension of ETMF films can only be determined from OMCTS and DMCPS measurements. The average is γ_{sv}=11.00 mJ/m^2, in agreement with the value reported for the annealed spin-coated ETMF films, i.e., 11.08 mJ/m^2 [20].

Contact angle deviations from the smooth curve of γ_{sv}=11.00 mJ/m^2

Figure 4 shows the $\gamma_{lv}\cos\theta$ vs γ_{lv} plot for the liquids listed in Table 2. The smooth curve corresponds to γ_{sv}=11.00 mJ/m^2 and β=0.000125 (mJ/m^2)$^{-2}$. This β is an average value that was obtained previously from contact angle results on different polymers [9]. The two points on the curve shown by triangles represent OMCTS and DMCPS. There are deviations in the contact angles of other liquids from this curve, ranging from ~−2.2° for *p*-xylene to ~−5.4° for methyl salicylate, as given in Table 5. The minus sign indicates that the experimental point is located above the curve. The corresponding errors in the calculated solid surface tension values are also given. Similar to the results for EGC-1700, contact angles of the test liquids fall above the γ_{sv}=11.00 mJ/m^2 curve, implying that the solid–liquid interfacial tension (γ_{sl}) in these systems is less than its ideal value. These findings confirm the view that arrangement of chains of a polymer film may be changed due to contact with a noninert liquid. Such a change can take place in the form of fluctuation of side chains (as for ETMF) or perturbation/rearrangement of polymer chains (as for EGC-1700) [19]. Therefore, inertness of the test liquid is necessary to prevent specific solid–liquid interactions and, thus, to determine the surface tension of a polymer film.

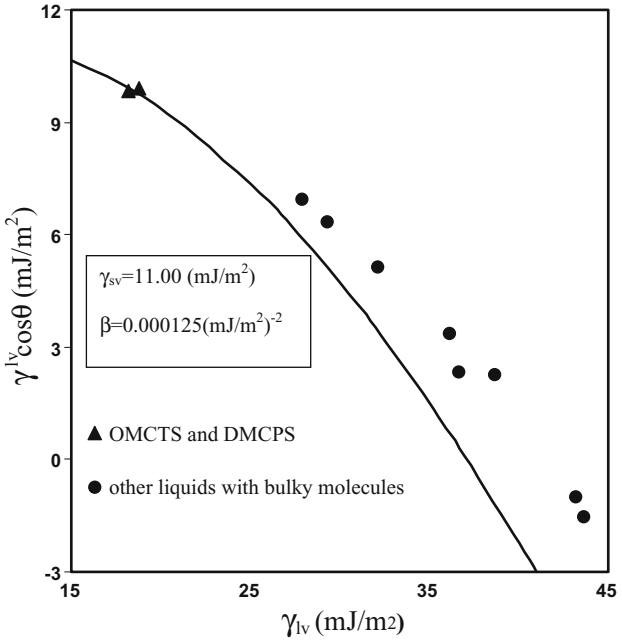

Fig. 4 Contact angle deviations from the smooth curve of γ_{sv}=11.00 mJ/m^2 (ETMF surface tension)

Table 4 Contact angle hysteresis for OMCTS and DCMPS on ETMF films

Liquid	$\theta^{o}_{hyst.}$ (°)
OMCTS	3.0
DMCPS	3.5

Comparison of the structure–property relationship between ETMF and EGC-1700

Time dependence of receding angles on ETMF films has most probably a different cause than for EGC-1700. Although the overall structure of the two polymers may seem to be fairly similar, two major differences should be noted: (a) in addition to the butyl and amide groups, ETMF possesses a much longer side chain, i.e., perfluoroheptyl compared to the perfluoropropyl side chain in EGC-1700; (b) unlike in the case of EGC-1700, which is an amorphous

Table 5 Deviation in the contact angles of the liquids with bulky molecules from the smooth curve of γ_{sv}=11.00 mJ/m^2 (ETMF) and the corresponding errors in the calculated solid surface tension values

Liquid	$\Delta\theta$ (°)	$\Delta\gamma_{sv}$ (mJ/m^2)
p-Xylene	−2.17	0.62
o-Xylene	−2.40	0.71
cis-Decalin	−3.04	0.95
Tetralin	−4.21	1.42
Diethyl phthalate	−3.09	1.05
Methyl salicylate	−5.41	1.94
Lepidine	−5.14	1.91
1-Bromonaphthalene	−4.95	1.87

fluorinated acrylate polymer, the H-bonding interactions within the perfluorinated amide groups in ETMF support formation of a layered structure in the bulk and on the top layer of the surface film. Molecular modeling and Wide Angle X-ray Spectroscopy (WAXS) measurements confirmed the existence of a layered structure for ETMF with a 3.5-nm distance between the two main chains [20]. In view of this, it seems less likely that the ETMF chains undergo a major reorientation/perturbation, as do chains of EGC-1700 upon contact with noninert liquids [19]. Comparing the extrapolated receding angles and the contact angle hysteresis for the liquids with bulky molecules on the two polymers elucidates this point. As seen in Table 6, a smaller hysteresis is obtained on ETMF surfaces in all cases. Furthermore, even those liquids that show slip-stick on the EGC-1700 films yield a smooth motion on ETMF surfaces. These results imply that compared to EGC-1700, the longer fluorinated side chains in ETMF provide a better shield around the hydrophilic backbone, reducing the specific solid–liquid interactions. The smaller solid surface tension of ETMF, i.e., 11.00 mJ/m^2 compared to 13.84 mJ/m^2 for EGC-1700, also confirm this view. It is suggested that sorption, retention, and mobility of side chains are the main contributors to the time dependence of receding angles of the test liquids on ETMF surfaces, as shown in Table 3.

Surface tension of ODMF films from contact angle measurements

Contact angles of the probe liquids on ODMF surfaces are shown in Table 7. Surprisingly, only OMCTS and DMCPS yielded useful contact angles. All other liquids either dissolved the polymer film or showed a slip-stick pattern. This implies an essential difference in the surface properties of ODMF and ETMF films, which is caused by the difference in their molecular composition. Both polymers have an alternating main chain structure possessing a 4-*N*-(perfluoroheptylcarbonyl)aminobutyl side chain. In addition, ODMF possesses a second *n*-hexadecyl side chain in the alternating main chain. According to the angle-dependent XPS investigations of the annealed ODMF surfaces, the presence of *n*-hexadecyl side chains suppresses good self-organization of the perfluoroalkyl side chains on the topmost layer of the film [20]. This specific structure–property relationship supports only a weak self-organization of the perfluoroalkyl side chains on the topmost layer of ODMF films. Moreover, the AFM analysis of ETMF and ODMF films also revealed that unlike ETMF films that are quite homogeneous, the *n*-hexadecyl and perfluoroalkyl side chains of ODMF undergo a weak phase separation, giving rise to a chemically heterogeneous film (Tavana et al., unpublished data).

The siloxane-based probe liquids, OMCTS and DMCPS, do not show specific interactions with the side chains of ODMF in the contact angle experiments. In contrast, other liquids that are hydrocarbon derivatives interact with the nonfluorinated parts of the film, resulting in slip-stick behavior or dissolution of the ODMF films. The above discussion suggests calculating the surface tension of ODMF from contact angles of OMCTS and DMCPS. To check if the calculation was correct, the receding contact angles and contact angle hysteresis of the two liquids were also investigated. Both liquids yield time-independent receding angles and small contact angle hysteresis on ODMF films (see Table 8), indicating that they do not penetrate into the polymer film nor do they cause a change in the configuration of the polymer chains. Thus, the surface tension of ODMF was determined to be γ_{sv}= 11.70 mJ/m^2. This value is fairly close to that reported for the

Table 6 Extrapolated receding contact angles and contact angle hysteresis for liquids with bulky molecules on ETMF and EGC-1700 surfaces

Liquid	ETMF		EGC-1700	
	θ_r^o (°)	$\theta_{hyst.}^o$ (°)	θ_r^o (°)	$\theta_{hyst.}^o$ (°)
p-Xylene	71.5	4.1	–	–
o-Xylene	74.0	3.5	–	–
cis-Decalin	77.2	3.7	64.3	8.5
Tetralin	80.0	4.7	54.6	22.0
Diethyl phthalate	76.4	10.0	45.0	30.0
Methyl salicylate	76.8	9.4	–	–
Lepidine	81.9	9.5	–	–
1-Bromonaphthalene	83.0	9.1	62.0	22.0

EGC-1700 poly(2,2,3,3,4,4,4-heptafluorobutyl methacrylate)

Table 7 Advancing contact angles of liquids with bulky molecules on ODMF surfaces

Liquid	θ_a (°)	γ_{sv} (mJ/m^2)	Comment
OMCTS	53.60±0.16	11.68	
DMCPS	55.19±0.08	11.72	
p-Xylene	–	–	Polymer dissolution
o-Xylene	–	–	Polymer dissolution
cis-Decalin	–	–	Slip-stick
Tetralin	–	–	Polymer dissolution
Methyl salicylate	–	–	Polymer dissolution
Lepidine	–	–	Polymer dissolution
1-Bromonaphthalene	–	–	Slip-stick

ODMF poly(octadecene-*alt*-*N*-(4-(perfluoroheptylcarbonyl)aminobutyl)maleimide)

Table 8 Contact angle hysteresis for OMCTS and DMCPS on ODMF surfaces

Liquid	$\theta_{hyst.}$ (°)
OMCTS	3.4
DMCPS	3.9

annealed spin-coated ODMF films, i.e., γ_{sv}=12.32 mJ/m^2 [20].

It should be noted that the surface tension of ODMF films is 0.7 mJ/m^2 larger than that of ETMF surfaces. This suggests that in addition to the perfluoroalkyl side chain, the *n*-hexadecyl side chain of ODMF is also present on the top of surface film, in agreement with the results reported earlier [20].

Receding angles and contact angle hysteresis

As discussed above, the contact angle hysteresis (θ^0_{hyst}) on ETMF films for the liquids containing electronegative atoms, oxygen or nitrogen, is about twice as large as for those with molecules that contain unsaturated bonds. It might be argued that the slope of the extrapolated lines may be different such that a larger θ^0_{hyst} is obtained in the former cases (e.g., in Fig. 3a). However, a closer evaluation shows that the differences in slope are not significant. Therefore, there must be a different cause for the difference in the contact angle hysteresis results in Table 3. At point (1) in Fig. 3a, when the motor is reversed to retract the drop, the drop front hinges to the solid surface, and the contact angles decrease very fast as more liquid is pumped out. Then the drop front starts moving back at point (2). Retreating the drop from (2) to (3) yields the receding angles, which decrease slowly with contact time. It is suggested that two different mechanisms are responsible for the trends shown in this figure: a fast process between points (1) and (2) giving rise to the contact angle hyseresis and a much slower process from (2) to (3) causing the receding angles to be time-dependent. The slower process was studied extensively on the fluoropolymer FC-732 films [29]. Liquid sorption/retention was suggested as the operative mechanism, decreasing the hydrophobicity of the film. Therefore, the receding angles decrease with the solid–liquid contact time. Considering that the slope of the regression lines is not significantly different for the liquids as in Table 3, the primary cause for the contact angle hysteresis appears to be the faster process (1–2). The fast process might have different causes. For example, the study of contact angles on EGC-1700 suggested reorientation/perturbation of the polymer chains due to contact with the test liquids as the dominant process [19]. However, this is less likely to happen to ETMF due to the shielding effect of the perfluoroheptyl segment around the chain. The fact that ETMF has a layered structure supported by the H-bonds within the chains confirms this claim. Two possible explanations for the contact angle hysteresis of the liquids in Table 3 are as follows: (1) because of mobility of the long side chains, the butyl or amide groups from side chain appear on the top of the surface film and interact with the liquid molecules; (2) liquid molecules can penetrate into the ETMF film, interacting with the hydrophilic groups of the chains. Whichever the case, such interactions are certainly stronger for the liquids containing electronegative moieties compared to those liquids with unsaturated bonds. This results in a stronger resistance to the motion of the drop front of the former liquids and hence larger contact angle hysteresis. To some extent, these two processes might also occur concurrently, and making a distinction between them is probably not possible.

It should be noted that if there were no contact angle hysteresis in a solid–liquid system, a single horizontal line would be obtained representing both the advancing and receding contact angles, when plotted as a function of time. Such a situation is reported for the contact angles of water on *n*-hexatriacontane ($C_{36}H_{74}$) films [31]. The chains were so well-packed that water molecules could not penetrate them nor did they show specific interactions with the solid molecules. Thus, when both of the processes discussed above were eliminated, a hysteresis-free system was obtained. More insight into the contributing effects could be gained by a systematic study of the contact angle hysteresis with a controlled rate of motion for the three-phase line.

OMCTS and DMCPS: suitable probe liquids

An extensive study of contact angle measurements with 28 liquids of various properties [a series of *n*-alkanes [11, 19] (Tavana et al., unpublished data) and liquids with bulky molecules] on four fluoropolymers with distinct chemical compositions in the backbone and the side chains suggests that OMCTS, DMCPS, and similar liquids with larger siloxane rings (e.g., dodecamethylcyclohexasiloxane and tetradecamethylcyclopentasiloxane) are the most suitable probe liquids to characterize the surface energetics of low-energy fluoropolymers. Contributing factors are:

1. The vapor pressure of these liquids is extremely low so that vapor adsorption onto the polymer film is eliminated.
2. The bulkiness of the molecules (e.g., the mean diameter for OMCTS is 0.9 nm) prevents penetration of the liquid into the polymer film.
3. The rigidity and non-flexibility of the molecules do not allow the solid to restructure them significantly at the surface.
4. The molecules are completely inert—without unsaturated bonds or exposable electronegative moieties—and do not show specific interactions with polymer films, e.g., slip-stick of the three-phase line, perturbation of polymer chains upon contact with the liquid, and dissolution of the polymer film.

Conclusion

Accurate surface tensions of low-energy fluorinated maleimide copolymers ETMF and ODMF are 11.00 and 11.70 mJ/m^2. A group of noninert liquids showed specific interactions with the molecular chains of these fluoropolymers, giving rise to different phenomena such as slip-stick of the liquid on the polymer surface and dissolution of the polymer film in case of ODMF, penetration of liquid molecules into the polymer film, and fluctuation of the long side chains in case of ETMF. On the other hand, due to the inertness of OMCTS and DMCPS molecules, their contact angles were used to determine the accurate surface tension of the polymer films. These two liquids are suitable for characterizing low-energy fluoropolymers because they do not interact with the polymer films in a specific fashion.

Acknowledgements This work was supported by the Natural Science and Engineering Research Council (NSERC) of Canada under grant no. 8278, University of Toronto Fellowship (H.T), and Ontario Graduate Scholarship (H.T).

References

1. Young T (1805) Philos Trans R Soc Lond 95:65
2. Zisman WA (1964) Contact angle, wettability and adhesion. In: Advances in chemistry. American Chemical Society, Washington, DC, p 43
3. Fowkes FM (1964) Ind Eng Chem 12:40
4. Driedger O, Neumann AW, Sell PJ (1965) Kolloid-Z Z Polym 201:52
5. Spelt JK, Li D (1996) In: Neumann AW, Spelt JK (eds) Applied surface thermodynamics, 1st edn. Dekker, New York, pp 239–292
6. Owens DK, Wendt RC (1969) J Appl Polym Sci 13:1741
7. van Oss CJ, Chaudhury MK, Good R (1988) J Chem Res 88:927
8. Good RJ, van Oss CJ (1992) In: Schrader M, Loeb G (eds) Modern approaches to wettability: theory and applications. Plenum, New York, pp 1–27
9. Li D, Neumann AW (1992) J Colloid Interface Sci 148:190
10. Kwok DY, Neumann AW (1999) Adv Colloid Interface Sci 81:167
11. Tavana H, Lam CNC, Friedel P, Grundke K, Kwok DY, Hair ML, Neumann AW (2004) J Colloid Interface Sci 279:493
12. Tavana H, Petong N, Hennig A, Grundke K, Neumann AW (2005) J Adhes 81:29
13. Tavana H, Gitiafroz R, Hair ML, Neumann AW (2004) J Adhes 80:705
14. Balasubramanian S, Klein M, llja Siepmann J (1995) J Chem Phys 103:3184
15. He M, Blum AS, Overney G, Overney R (2002) Phys Rev Lett 88:154302
16. Christenson HK, Gruen DWR, Horn RG, Israelachvili JN (1989) J Chem Phys 87:1834
17. Ribarsky MW, Landman U (1992) J Chem Phys 97:1937
18. Landman U, Xia T, Ouyang J, Ribarsky MW (1992) Phys Rev Lett 69:1967
19. Tavana H, Simon F, Grundke K, Kwok DY, Hair ML, Neumann AW (2005) J Colloid Interface Sci 291:497
20. Appelhans D, Wang Z-G, Zschoche S, Zhuang R-C, Häussler L, Friedel P, Simon F, Jehnichen D, Grundke K, Eichhorn K-J, Komber H, Voit B (2005) Macromolecules 38:1655
21. Lahooti S, Del Rio OI, Cheng P, Neumann AW (1996) In: Neumann AW, Spelt JK (eds) Applied surface thermodynamics, 1st edn. Dekker, New York, pp 441–507
22. Holmes-Farley SR, Reamey RH, Nuzzo R, McCarthy TJ, Whitesides M (1987) Langmuir 3:799
23. Yasuda T, Okuno T, Yoshida K, Yasuda H (1988) J Polym Sci 26:1781
24. Yasuda T, Miyama M, Yasuda H (1994) Langmuir 10:583
25. Lavielle L, Schultz J (1985) J Colloid Interface Sci 106:438
26. Ruckenstein E, Gourisankar SV (1985) J Colloid Interface Sci 107:488
27. Yasuda T, Miyama M, Yasuda H (1992) Langmuir 8:1425
28. Wang JH, Claesson PM, Parker JL, Yasuda H (1994) Langmuir 10:3897
29. Lam CNC, Kim N, Hui D, Kwok DY, Hair ML, Neumann AW (2001) Colloids Surf A Physicochem Eng Asp 189:265
30. Hennig A, Eichorn K-J, Staudinger U, Sahre K, Rogalli M, Stamm M, Neumann AW, Grundke K (2004) Langmuir 20:6685
31. Neumann AW (1974) Adv Colloid Interface Sci 4:105